Metal Pyrazolato Complexes. Synthesis, Characterization, and X-ray Powder Diffraction Studies of Group 12 Coordination Polymers

Norberto Masciocchi,*,†,§ G. Attilio Ardizzoia,*,‡,§ Angelo Maspero,‡ Girolamo LaMonica,‡,§ and Angelo Sironi†

Dipartimento di Chimica Strutturale e Stereochimica Inorganica e Centro CNR, Università di Milano, Via Venezian 21, 20133 Milano, Italy, Dipartimento di Chimica Inorganica, Metallorganica, ed Analitica e Centro CNR, Università di Milano, Via Venezian 21, 20133 Milano, Italy, and Dipartimento di Scienze Chimiche, Fisiche e Matematiche, Università dell'Insubria, via Lucini 3, 22100 Como, Italy

Received March 3, 1999

A number of polymeric pyrazolato complexes have been prepared and characterized by spectroscopy, thermal analyses (DSC and TGA), and X-ray powder diffraction (XRPD) methods. Ab initio XRPD studies showed that the (isomorphous) $[Zn(pz)_2]_n$ and $[Cd(pz)_2]_n$ species (Hpz = pyrazole) are 1-D polymers containing tetrahedrally coordinated metals and $M(\mu\text{-pz})_2M$ (M = Zn, Cd) bridges, much alike $[Cu(pz)_2]_n$ [orthorhombic, *Ibam*, a = 7.4829(4), b = 14.3844(6), c = 7.3831(3) Å (Zn) and a = 7.8591(6), b = 13.652(1), c = 7.9165(4) Å (Cd)]; differently, $Hg(pz)_2$ [triclinic, $P\bar{1}$, a = 7.4097(3), b = 9.4474(3), c = 5.8345(3) Å, α = 96.310(2), β = 96.752(3), and γ = 73.694(2)°] is best described as a mononuclear complex, containing two *monodentate* pyrazolato ligands loosely interacting, through long(er) Hg···N contacts with neighboring molecules. During the synthesis of the latter, an intermediate phase was obtained, and characterized as $Hg(pz)NO_3$, which contains a polymeric polycation, $[Hg(pz)]_n^{n+}$, based on $Hg(\mu\text{-pz})Hg$ bridges, and uncoordinated NO_3^- groups (orthorhombic, *Pcmn*, a = 17.2985(9), b = 5.2538(3), c = 7.3912(4) Å). All structures were ultimately refined by the Rietveld method.

Introduction

In recent years, there has been a growing interest in preparing and characterizing coordination polymers for their possible application in a number of different fields; indeed, some metal-containing polymeric species have been shown to be photochemically active or to possess interesting electrical, electrochemical, magnetic, or SHG properties,[1] and even antimicrobial activity.[2] Such polymers typically contain a backbone of transition metal ions in close proximity, joined by polydentate ligands.[3] In this respect, the pyrazolato anion (and its ring-substituted derivatives) has proved to be an excellent synthon since, in the vast majority of its metal complexes, it acts, in the common *exo*-bidentate coordination mode, as a four-electron donor ligand on two metals at distances in the 3.3−3.8 Å range.[4]

We have recently been interested in the coordination chemistry of polynuclear complexes containing pyrazolato ligands and a number of transition metals such as Cu, Ag, Pd, and Re,[5] the main objective of such studies residing in the discovery and characterization of the catalytical aspects of their reactivity. On top of such studies, we also characterized the crystallochemical properties of several binary (homoleptic) Group 11 diazolato species (precursors of the catalytic ones), and surprisingly discovered a wide variety of polynuclear arrangements, ranging from trimers, tetramers, and hexamers up to polymeric species, that could be selectively prepared and isolated.[6] Since most of such species are insoluble and cannot be obtained as single crystals of suitable quality, the main body of the structural studies performed so far have been based on the newly emerging technique of ab initio X-ray powder diffraction crystal structure determination,[7] which allowed a complete characterization of new and unexpected features, such as the presence of polymor-

* Corresponding author. Tel: +39 02 70635120. Fax: +39 02 70635288. E-mail: norbert@csmtbo.mi.cnr.it.

† Università di Milano, Chimica Strutturale.

‡ Università di Milano, Chimica Inorganica.

§ Università dell'Insubria, on leave.

(1) (a) Mark, J, E.; Allcock, H. R.; West, R.; *Inorganic Polymers*; Prentice Hall: Englewood Cliffs, NJ, 1992. (b) *Inorganic and Organometallic Polymers II*; Wisian-Neilson, P., Allcock, H. R., Wynne, K. J., Eds.; ACS Symposium Series 572, American Chemical Society: Washington, DC, 1994.

(2) *The Agrochemicals Handbook*, 3rd ed.; Kidd, H., James, D. R., Eds.; Royal Society of Chemistry Information Services: Cambridge, UK, 1991. (b) For recent examples of silver diazolates see: Nomiya, K.; Tsuda, K.; Sudoj, T.; Oda, M. *J. Inorg. Biochem.* **1997**, *68*, 39−44.; Nomiya, K.; Tsuda, K.; Kasuga, N. C. *J. Chem. Soc., Dalton Trans.* **1998**, 1653−1659.

(3) McCleverty, J. A.; Ward, M. D. *Acc. Chem. Res.* **1998**, *31*, 842−851.

(4) LaMonica, G.; Ardizzoia, G. A. *Prog. Inorg. Chem.* **1997**, *46*, 151−238.

(5) (a) Ardizzoia, G. A.; Angaroni, M. A.; LaMonica, G.; Cariati, F.; Moret, M.; Masciocchi, N. *J. Chem. Soc., Chem. Commun.* **1990**, 1021−1023. (b) Ardizzoia, G. A.; Angaroni, M. A.; LaMonica, G.; Cariati, F.; Cenini, S.; Moret, M.; Masciocchi, N. *Inorg. Chem.* **1991**, *30*, 4347−4353. (c) Ardizzoia, G. A.; Cenini, S.; LaMonica, G.; Masciocchi, N.; Moret, M. *Inorg. Chem.* **1994**, *33*, 1458−1463. (d) Masciocchi, N.; Moret, M.; Sironi, A.; Ardizzoia, G. A.; LaMonica, *J. Chem. Soc., Chem. Commun.* **1995**, 1955−1956. (e) Ardizzoia, G. A.; LaMonica, G.; Maspero, A.; Moret, M.; Masciocchi, N. *Inorg. Chem.* **1997**, *36*, 2321−2328. (f) Ardizzoia, G. A.; LaMonica, G.; Maspero, A.; Moret, M.; Masciocchi, N. *Eur. J. Inorg. Chem.* **1998**, 1503−1512.

(6) (a) Masciocchi, N.; Moret, M.; Cairati, P.; Sironi, A.; Ardizzoia, G. A.; LaMonica, G.; Cenini, S. *J. Am. Chem. Soc.* **1994**, *116*, 7668−7676. (b) Masciocchi, N.; Cairati, P.; Sironi, A. **1998**, *13*, 35−40. (e) Ardizzoia, G. A.; Cenini, S.; LaMonica, G.; Masciocchi, N.; Maspero, A.; Moret, M. *Inorg. Chem.* **1998**, *37*, 4284−4292.

(7) (a) Harris, K. D. M.; Tremayne, M. *Chem. Mater.* **1996**, *8*, 2554−2570. (b) Langford, J. I.; Louër, D. *Rep. Prog. Phys.* **1996**, *59*, 131−234. (c) Masciocchi, N.; Sironi, A. *J. Chem. Soc., Dalton Trans.* **1997**, 4643−4650. (d) Poojary, D. M.; Clearfield, A. *Acc. Chem. Res.* **1997**, *30*, 414−422.

10.1021/ic990258u CCC: $18.00
Published on Web 07/13/1999

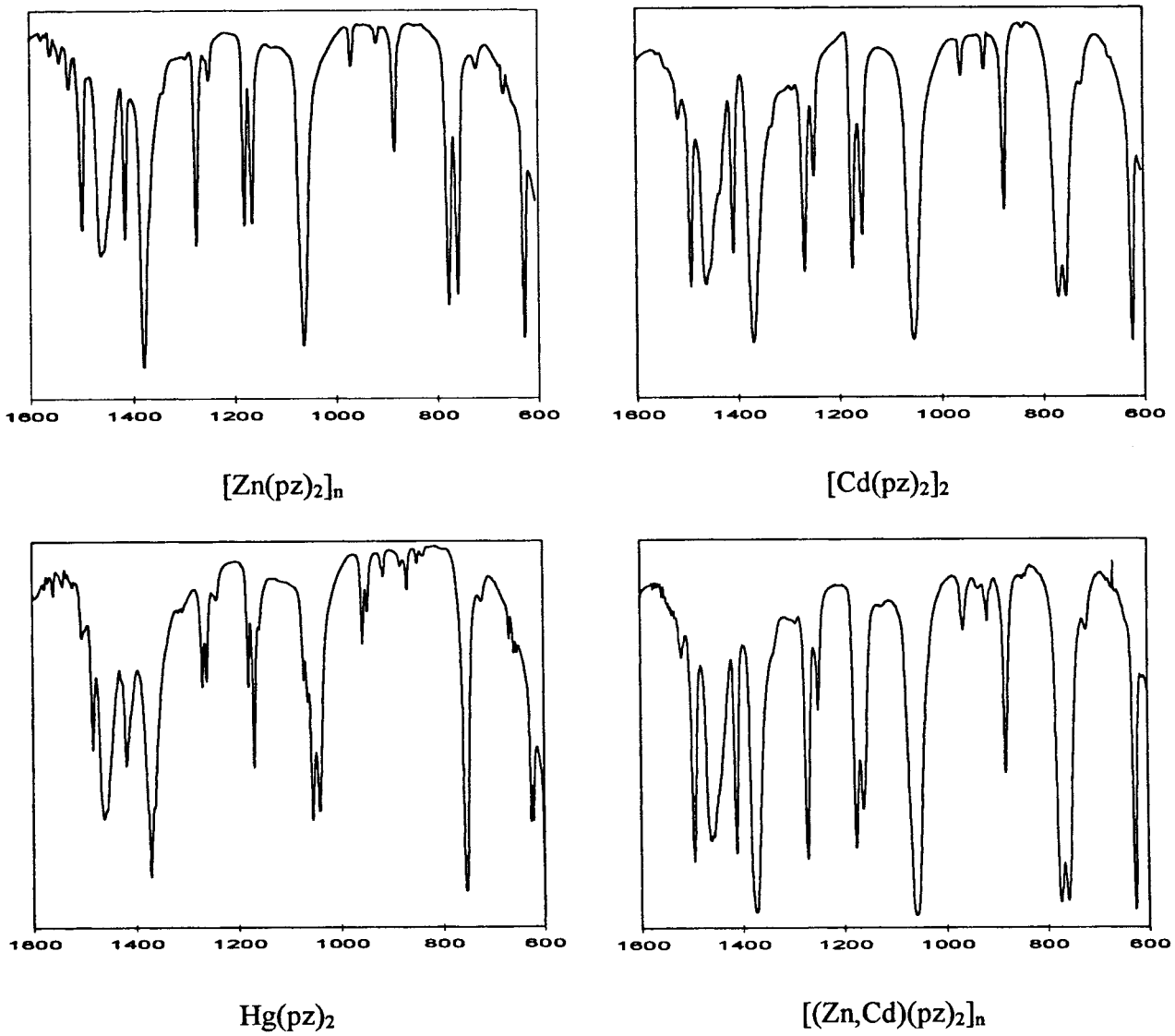

Figure 1. Plot of the IR spectra (Nujol mulls) for group 12 metal pyrazolates, in the 1600−600 cm^{-1} range.

phic behavior,[8] the reversibility of ring-opening polimerization reactions,[9] and ordered cocrystallization of hexanuclear and polymeric moieties within the same crystal lattice.[10]

With the aim of extending our studies and methodology to new, but related, species, we have undertaken the synthesis and structural, spectroscopical, and thermal characterization of pyrazolato complexes of Group 12 metals. Indeed, robust one-dimensional polymers containing zinc atoms bridged by aromatic heterocycles have been very recently proven to possess interesting photoluminescent properties, while "*The insoluble and intractable nature of these species ... enables their usage in a variety of semiconducting applications*".[11] The results presented heareafter complement and correct a number of conflicting reports of poorly characterized metal pyrazolates, somewhat scattered in the scientific literature.[12]

(8) Masciocchi, N.; Ardizzoia, G. A.; LaMonica, G.; Moret, M.; Sironi, A. *Inorg. Chem.* **1997**, *36*, 449−454.
(9) Masciocchi, N.; Corradi, E.; Moret, M.; Ardizzoia, G. A.; Maspero, A.; LaMonica, G.; Sironi, A. *Inorg. Chem.* **1997**, *36*, 5648−5650.
(10) Masciocchi, N.; Ardizzoia, G. A.; LaMonica, G.; Maspero, A.; Sironi, A. *Angew. Chem., Int. Ed.* **1998**, *37*, 3366−3369.
(11) Thomsen, L. T.; Papadimitrakopoulos, F. *Macromol. Symp.* **1997**, *125*, 143−150.
(12) (a) Vos, J. G.; Groeneveld, L. W. *Inorg. Chim. Acta* **1977**, *24*, 123−126. (b) Das, M. K.; Ghosh, S. *Indian J. Chem.* **1997**, *36A*, 324−327.

Experimental Section

General. Pyrazole (Hpz) and metal salts were used as supplied (Aldrich Chemical Co.). Solvents were dried and distilled by standard methods. Infrared spectra (see Figure 1) were recorded on a Bio-Rad FTIR 7 instrument. Thermogravimetric analyses were performed on a Perkin-Elmer TGA-7 system. DSC traces were obtained with the aid of a Perkin-Elmer DSC 7 calorimeter. Elemental analyses (C, H, N) were carried out at the Microanalytical Laboratory of the University of Milan.

Synthesis of $[Zn(pz)_2]_n$, 1. To a solution of $ZnCl_2$ (1.00 g, 7.33 mmol) in water (25 mL), pyrazole (1.50 g, 22.1 mmol) was added under stirring. The clear solution was stirred at room temperature for about 5 min and then NH_3 (0.5 mL, 25% w/w water solution) was added. The white suspension formed was stirred for 30 min. at room temperature. The solid was then filtered, washed with water and methanol, and dried under vacuum (1.41 g, 96%). $Zn(ClO_4)_2$ or $Zn(NO_3)_2$ can be also employed in place of zinc chloride. Anal. Calcd for $C_6H_6N_4Zn$: C, 36.11; H, 3.01; N, 28.09. Found: C, 35.94; H, 2.86; N, 27.87. Main IR bands (Nujol mulls, cm^{-1}): 3122 w, 3109 w, 1498 m, 1415 m, 1379 s, 1275 w, 1250 w, 1180 m, 1165 m, 1064 s, 969 w, 919 w, 884 m, 778 m, 759 m, 627 m.

Synthesis of $[Cd(pz)(OH)]_n$. To a solution of $CdCl_2$ (1.00 g, 5.45 mmol) in water (25 mL), pyrazole (1.11 g, 16.3 mmol) was added under stirring. A white precipitate, identified as $[Cd(Hpz)_2Cl_2]$, suddenly formed. The suspension was stirred for about 10 min and then NH_3 (0.5 mL, 25% w/w water solution) was added. After 30 min the white

solid was filtered off, washed with methanol and dried under vacuum (1.01 g, 94%). Anal. Calcd for $C_3H_4CdN_2O$: C, 18.36; H, 2.03; N, 14.25. Found: C, 18.41; H, 2.12; N, 14.73. Main IR bands (Nujol mulls, cm^{-1}): 3406 s, 3106 w, 3095 w, 3087 w, 1486 w, 1410 m, 1363 s, 1265 w, 1247 m, 1161 m, 1141 w, 1043 m, 946 w, 772 s, 760 s, 681 w, 632 m.

Synthesis of $[Cd(Hpz)(pz)_2]_2$. CdO **(**500 mg, 3.84 mmol) and pyrazole (5.30 g, 77.9 mmol) were heated at 180 °C in a sealed flask under nitrogen, without stirring, until the yellowish color of cadmium oxide disappeared (about 5 h). The mixture was then allowed to cool and solidify, giving a white solid. The residue was then washed with acetone in order to eliminate excess pyrazole and finally filtered giving 1.14 g (93% yield) of $[Cd(Hpz)(pz)_2]_2$. Anal. Calcd for $C_9H_{10}CdN_6$: C, 34.35; H, 3.18; N, 26.72. Found: C, 33.89; H, 3.34; N, 26.34. Main IR bands (Nujol mulls, cm^{-1}): 3382 s, 3135 w, 3121 w, 3108 w, 3099 w, 3086 w, 1522 w, 1487 m, 1410 m, 1371 m, 1248 m, 1168 m, 1157 m, 1117 m, 1047 s, 1031 s, 909 w, 880 w, 770 s, 756 s, 674 m, 630 m.

Synthesis of $[Cd(pz)_2]_n$, 2. (a) Complex $[Cd(Hpz)(pz)_2]_2$ (500 mg, 1.59 mmol) was placed in a sublimation apparatus and heated to 300 °C by means of an heat gun, controlling the temperature (±5 °C) by employing a standard thermocouple. Condensation of solid pyrazole was observed on the coldfinger of the apparatus. After 30 min heating was stopped. The solid was allowed to cool and was then removed, washed with acetone, and dried under vacuum (385 mg, 98%); b) to a solution of $CdCl_2$ **(**1.00 g, 5.45 mmol) in water (30 mL), pyrazole (2.25 g, 33.1 mmol) was added under stirring. The clear solution was stirred at room temperature for about 5 min, and then NH_3 (0.5 mL, 25% w/w water solution) was added. The white suspension formed was stirred for 30 min at room temperature. The solid was then filtered, washed with water and methanol, and dried under vacuum (1.24 g, 92%). $Cd(ClO_4)_2$ can equally be employed in place of cadmium chloride. Anal. Calcd for $C_6H_6CdN_4$: C, 29.21; H, 2.44; N, 22.72. Found: C, 28.87; H, 2.21; N, 22.86. Main IR bands (Nujol mulls, cm^{-1}): 3122 w, 3102 w, 1492 m, 1410 m, 1370 s, 1269 w, 1250 w, 1175 m, 1156 m, 1055 s, 960 w, 915 w, 877 m, 769 m, 756 m, 624 m.

Synthesis of $[Hg(pz)(NO_3)]_n$, 3. To 25 mL of a filtered saturated solution of $Hg(NO_3)_2$ in acetonitrile [about 200 mg of $Hg(NO_3)_2$, 0.62 mmol] was added pyrazole (126 mg, 1.85 mmol) under stirring. The formed suspension was stirred for 30 min, the solid was then filtered, washed with water and methanol, and dried under vacuum (197 mg, 96% yield). Anal. Calcd for $C_3H_3HgN_3O_3$: C, 10.92; H, 0.91; N, 12.74. Found: C, 10.69; H, 1.22; N, 12.77. Main IR bands (Nujol mulls, cm^{-1}): 3141 w, 3130 w, 3121 w, 1507 w, 1434 w, 1355 m, br, 1191 m, 1075 m, 909 w, 822 w, 763 m, 725 w, 620 w.

Synthesis of $Hg(pz)_2$, 4. To the aforementioned suspension, Et_3N (0.5 mL) was added dropwise. The consistency of the solid rapidly changed and a decrease of its volume was also observed. After 15 min stirring, the solid was filtered, washed with water and methanol, and dried under vacuum (202 mg, 98%). Anal. Calcd for $C_6H_6HgN_4$: C, 21.52; H, 1.79; N, 16.74. Found: C, 21.88; H, 1.91; N, 16.26. Main IR bands (Nujol mulls, cm^{-1}): 3133 w, 3120 w, 3107 w, 3094 w, 1485 m, 1418 m, 1371 m, 1270 m, 1261 m, 1181 m, 1169 m, 1072 m, 1065 sh, 1055 m, 1041 m, 956 w, 946 w, 914 w, 868 w, 755 s, 668 w, 626 m.

X-ray Powder Diffraction Analysis of 1, 2, 3, and 4. The powders were gently ground in an agate mortar, than cautiously deposited in the hollow of an aluminum holder equipped with a zero background plate (supplied by *The Gem Dugout*, State College, PA) with the aid of glass slide. The samples were rotated at about 60 rpm about the scattering vector, to improve particle statistics and to minimize preferred orientation effects.[13] Diffraction data (Cu Kα, $\lambda = 1.5418$ Å) were collected on a horizontal scan D III/Max Rigaku diffractometer, equipped with parallel (Soller) slits, a secondary beam curved graphite monochromator, a Na(Tl)I scintillation detector and pulse height amplifier discrimination. The generator was operated at 40 KV and 40 mA. Slits used: divergence 1.0°, antiscatter 1.0° and receiving 0.3 mm. Nominal resolution for the present setup is 0.14° 2θ (fwhm) for the Si(111) peak at 28.44° (2θ). Long overnight scans were performed with $5 < 2\theta < 105°$, with $t = 10$ s and $\Delta 2\theta = 0.02°$.

Indexing, using TREOR,[14] of the low angle peaks suggested, for **1** and **2**, I-centered orthorhombic cells of approximate dimensions $a = 7.48$ Å, $b = 14.38$ Å, $c = 7.39$ Å for **1** [M(15)[15] = 18; F(15)[16] = 24 (0.014, 45)] and $a = 7.92$ Å, $b = 13.64$ Å, $c = 7.92$ Å for **2** [*pseudo*tetragonal, M(11) = 13; F(11) = 9 (0.018, 72)]; differently, the unit cell determination lead to a primitive orthorhombic cell for **3** [$a = 17.27$ Å, $b = 5.24$ Å, $c = 7.38$ Å, M(17) = 36; F(17) = 51 (0.009, 39)] and to a triclinic lattice for **4** [$a = 7.38$ Å, $b = 9.43$ Å, $c = 5.83$ Å, $\alpha = 96.5°$, $\beta = 96.8°$, and $\gamma = 73.5°$; M(17) = 24; F(17) = 46 (0.016, 23)]. Systematic absences for **1** and **2** indicated *Ibam* as the probable space group, later confirmed by successful refinement; **3** was solved, and refined, in *Pcmn*, while centric $P\bar{1}$ was chosen for complex **4**.

Despite the lattice parameters of **1** and **2**, together with their space group symmetry, could have been indicative of the isomorphous character of such species with the already known $[Cu(pz)_2]_n$ phase (allowing to build the initial, approximate structural models for **1** and **2** from the published coordinates of the copper analogue, vide infra), we "solved" their structures by simple geometrical and packing considerations: indeed, in *Ibam*, the only crystallographic sites consistent with *four* $M(pz)_2$ molecules per unit cell *and* meaningful metal coordination geometry and connectivity are those of 222 symmetry. Geometrical modeling was then used to compute approximate coordinates for the C and N atoms of the pyrazolato ligands. Structure solution of **3** and **4** was initiated by extracting, using EXTRA,[17] 76 and 173 ($2\theta < 55°$) independent F_o's, respectively, which afforded easily interpretable Patterson maps and the approximate location of the mercury atoms. Difference Fourier syntheses and geometric modeling later afforded approximate coordinates for the remaining non-hydrogen atoms.

The final refinements were performed with the aid of the GSAS suite of programs,[18] by imposing steric constraints to chemically stiff and known fragments, such as the pz and NO_3 groups; pyrazolato ring and N−O bonds were given average literature values of 1.38 and 1.20 Å, respectively (internal ring angles being fixed at 108°, and planar trigonal geometry assumed for the nitrate). Soft restraints were also applied to Hg−N distances (2.15 Å in **3** and **4**). The peak shapes were best described by the Thompson/Cox/Hastings formulation[19] of the pseudo Voigt function, with GV and LY set to zero. The background functions were described by a cosine Fourier series, while systematic errors were corrected with the aid of a sample-displacement angular shift, and, for **1**, **2**, and **4**, a preferred orientation parameter, in the formulation of March and Dollase[20] (with 120, 120,[21] and 010 pole vectors, and coefficients equal to 0.78, 0.94, and 0.80, respectively). Metal atoms were given a refinable isotropic displacement parameter [U_{iso}(M)], while lighter atoms' U's were arbitrarily given [U_{iso}(M) + 0.02] Å^2 values. The contribution of the hydrogen atoms to the scattered intensity was neglected. Scattering factors, corrected for real and imaginary anomalous dispersion terms, were taken from the internal library of GSAS. Final R_p, R_{wp}, and R_F agreement factors, together with

(13) At least in the plane normal to the scattering vector. See for example: Parrish, W.; Huang, T. C. *Adv. X-ray Anal.* **1983**, *26*, 35−44.

(14) Werner, P. E.; Eriksson, L.; Westdahl, M. *J. Appl. Crystallogr.* **1985**, *18*, 367−370.
(15) De Wolff, P. M. *J. Appl. Crystallogr.* **1968**, *1*, 108−113.
(16) Smith, G. S.; Snyder, R. L. *J. Appl. Crystallogr.* **1979**, *12*, 60−65.
(17) Altomare, A., Burla, M. C.; Cascarano, G.; Giacovazzo, C.; Guagliardi, A.; Moliterni, A. G. G.; Polidori, G. *J. Appl. Crystallogr.* **1995**, *28*, 842−846.
(18) Larson, A. C.; Von Dreele, R. B. LANSCE, MS-H805, Los Alamos National Laboratory: Los Alamos, NM, 1990.
(19) Thompson, P.; Cox, D. E.; Hastings, J. B. *J. Appl. Crystallogr.* **1987**, *20*, 79−83.
(20) (a) March, A. *Z. Kristallogr.* **1932**, *81*, 285−297. (b) Dollase, W. A. *J. Appl. Crystallogr.* **1986**, *19*, 267−272.
(21) Conventional optical microscropy did not reveal, for any of the prepared polycrystalline species, clearly defined crystal morphologies, the typical grain size being lower than 10 μm. The odd, *experimentally determined*, 120 preferred orientation pole vector for compounds **1** and **2** is however in good agreement with a cleavage plane of pseudohexagonally packed chains of the orthorhombic crystals, running along [001].

Table 1. Crystal Data and Refinement Parameters for Compounds **1**, **2**, **3**, and **4**

	1	**2**	**3**	**4**
species	$[Zn(pz)_2]_n$	$[Cd(pz)_2]_n$	$Hg(pz)NO_3$	$Hg(pz)_2$
formula	$C_6H_6N_4Zn$	$C_6H_6CdN_4$	$C_3H_3HgN_3O_3$	$C_6H_6HgN_4$
fw, g mol^{-1}	199.81	246.54	329.66	334.73
cryst syst	orthorhombic	orthorhombic	orthorhombic	triclinic
space group	*Ibam*	*Ibam*	*Pcmn*	$P\bar{1}$
a, Å	7.4829(4)	7.8591(6)	17.2985(7)	7.4097(3)
b, Å	14.3844(6)	13.6520(10)	5.2538(3)	9.4473(3)
c, Å	7.3831(3)	7.9165(4)	7.3912(4)	5.8345(3)
α, deg	90	90	90	96.310(2)
β, deg	90	90	90	96.752(3)
γ, deg	90	90	90	73.694(2)
V, Å^3	794.70(4)	849.38(8)	671.73(8)	388.01(4)
Z	4	4	4	2
ρ_{calc}, g cm^{-3}	1.667	1.928	3.259	2.865
μ(Cu Kα), cm^{-1}	71.8	382.1	789.6	678.7
diffractometer		Rigaku D-III Max		
T, K	298	298	298	298
2*θ* range, deg	17−97	17−97	17−97	17−97
N_{obs}	4001	4001	4001	4001
N_{refl}	212	226	432	743
wR_p, R_p	0.132, 0.104	0.098, 0.077	0.110, 0.080	0.105, 0.081
R_F, χ	0.125, 3.00	0.066, 1.06	0.066, 3.21	0.058, 2.85

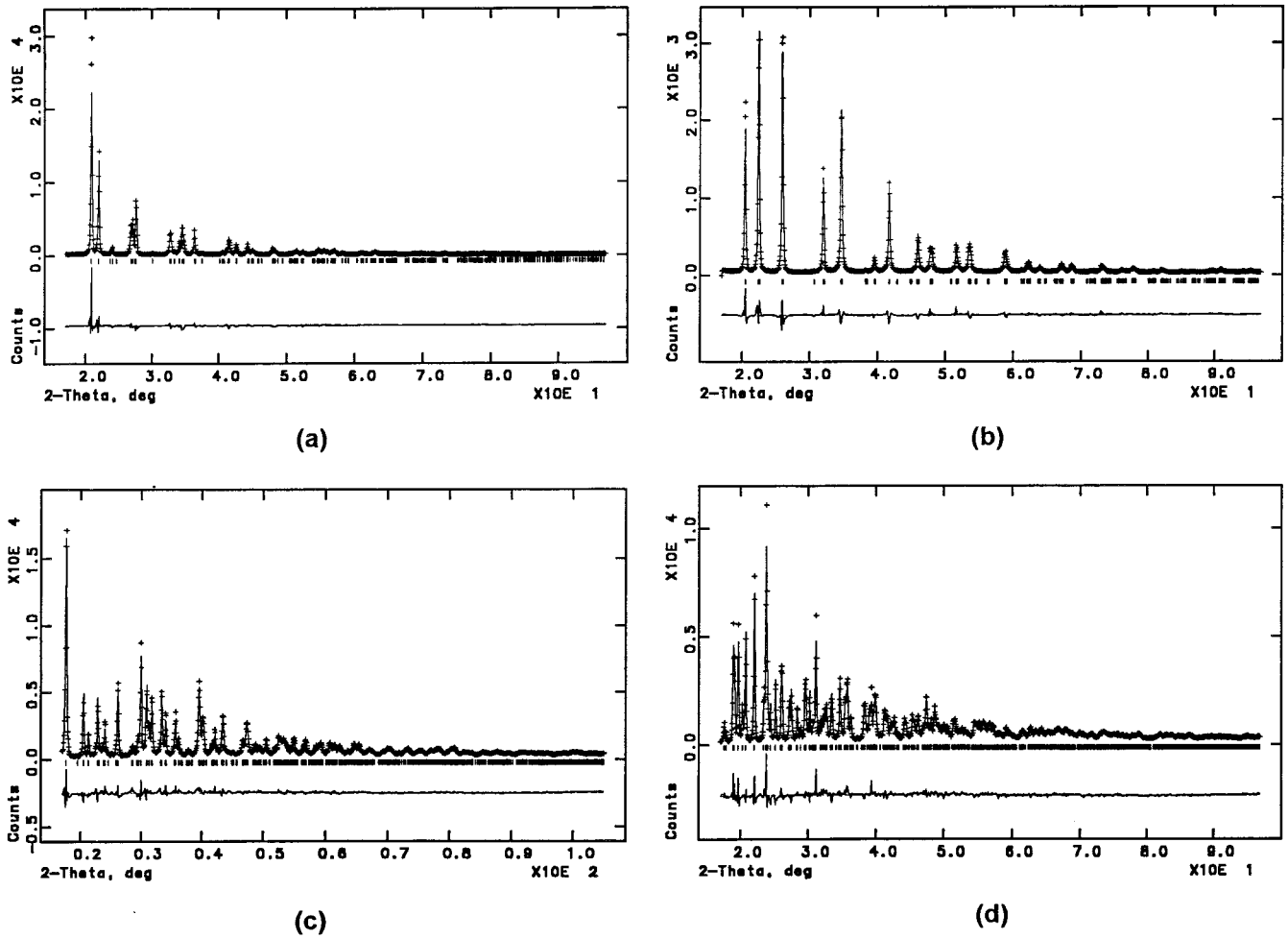

Figure 2. Rietveld refinement plots for **1**, **2**, **3**, and **4**. Difference plot and peak markers at the bottom.

details of the data collections and analyses for the four crystal phases can be found in Table 1. In the final cycles, data below 17° (2*θ*), i.e., those most affected by instrumental aberrations and incident beam overflow, were omitted; Figure 2a−d shows the final Rietveld refinement plots for **1**, **2**, **3**, and **4**, respectively. Final fractional coordinates and full lists of bond distances and angles are supplied as Supporting Information.

Results and Discussion

Synthesis. The aim of the synthetic approaches adopted in this work was 2-fold: first, to prepare analytically pure species and, second, to obtain samples in *microcrystalline* forms, suitable for an XRPD analysis and, therefrom, for their complete structural determination. The first task has been only partially

tackled by two groups, which independently reported the synthesis of group 12 binary metal−pyrazolate complexes.[12]

Zinc. The synthetic route employed by Vos and Groeneveld[12a] has been successfully adapted to the synthesis of $[Zn(pz)_2]_n$. When an aqueous solution of $ZnCl_2$ was treated with a 3-fold excess of pyrazole in the presence of NH_3, complex **1** was isolated in quantitative yields. $[Zn(pz)_2]_n$ can also be obtained by using different zinc salts, such as nitrate or perchlorate (eq 1).

$$ZnX_2 + 2Hpz \xrightarrow[-\ NH_4X]{NH_3} {}^1/_n[Zn(pz)_2]_n \ (X = Cl,\ NO_3,\ ClO_4) \quad (1)$$

According to this formulation the IR spectrum of **1** does not show any absorption attributable to N−H stretching. Moreover, and different from what was observed by Das and Ghosh[12b] (who, however, employed a different synthetic procedure), no coordinated water was evidenced.

Cadmium. The reaction of cadmium chloride with pyrazole follows a different pathway from that of $ZnCl_2$. When $CdCl_2$ was reacted with pyrazole (Cd/Hpz = 1:3) in water, the initial formation of $[Cd(Hpz)_2Cl_2]$[22] was observed. The addition to the reaction medium of an aqueous solution of NH_3 or NaOH causes the formation of a species exhibiting, in its IR spectrum, a quite sharp band of medium intensity centered at 3406 cm^{-1}. On the basis of this observation, and with the support of analytical data (see Experimental Section) we formulate this species as a hydroxo/pyrazolate complex of cadmium(II), i.e., $[Cd(OH)(pz)]_n$; the absence of significant peaks in the powder diffraction pattern of this (probably polymeric) species prevented, however, its structural characterization.

On heating $[Cd(OH)(pz)]_n$ at 240 °C, under N_2, the formation of CdO and $[Cd(pz)_2]_n$ was observed, as suggested by IR, XRPD, and TGA monitoring (eq 2):

$$ {}^2/_n[Cd(OH)(pz)]_n \xrightarrow{240\ °C} CdO + {}^1/_n[Cd(pz)_2]_n + H_2O \quad (2)$$

The formation of CdO can be explained by a condensation reaction of the pyrazolate ion with the hydroxyl moiety, as in (eq 3):[23]

$$ {}^1/_n[Cd(OH)(pz)]_n \rightarrow CdO + Hpz \quad (3)$$

Concerning the formation of $[Cd(pz)_2]_n$, a reasonable assumption was that it can be derived from the reaction between CdO and Hpz. To substantiate this hypothesis, and with the aim of obtaining $[Cd(pz)_2]_n$ in an analytically pure form, the reaction of CdO with molten pyrazole was carried out. Indeed, cadmium oxide reacts with pyrazole at 180 °C, allowing the selective formation of a new species, formulated (analytical and spectroscopic data) as the dinuclear pyrazole/pyrazolate $[Cd(Hpz)(pz)_2]_2$ complex [containing, beside the two neutral pyrazole ligands, two double-brigding (*exo*-bidentate) and two *mono*-dentate pyrazolate groups] (eq 4):

$$2CdO + 6Hpz \xrightarrow{180\ °C} [Cd(Hpz)(pz)_2]_2 + 2H_2O \quad (4)$$

The IR spectrum of $[Cd(Hpz)(pz)_2]_2$ shows a strong absorption at 3382 cm^{-1} attributable to the ν(N−H) of the neutral coordinated pyrazole molecules. The sharpness of this band excludes strong interactions (hydrogen bonds) between the pyrazolate and the pyrazole ligands, similar to those observed in a number of species complexes containing both pyrazolate groups and pyrazole molecules in sterically favorable environments.[24] Two other absorptions of medium intensity are observed at 1522 and 1485 cm^{-1} and can be assigned to the so-called ring breathing of the neutral and anionic heterocyclic rings, respectively.[25] The formulation presented above is also based on the analogy with a strictly related derivative, $[Zn(Hdmpz)(dmpz)_2]_2$ (Hdmpz = 3,5-dimethylpyrazole), synthesized from metallic zinc and Hdmpz at 90 °C under an oxygen atmosphere and structurally characterized.[26]

On heating $[Cd(Hpz)(pz)_2]_2$ at 300 °C under N_2, sublimation of free pyrazole was observed (as also quantitatively confirmed by thermogravimetric analyses), and the selective formation of $[Cd(pz)_2]_n$ was achieved (eq 5):

$$[Cd(Hpz)(pz)_2]_2 \xrightarrow{300\ °C} {}^2/_n[Cd(pz)_2]_n + 2Hpz \quad (5)$$

When the reaction between $CdCl_2$ and pyrazole is carried out with a large excess of pyrazole, the intermediate formation of the insoluble $[Cd(Hpz)_2Cl_2]$ was not observed, and the presence of Et_3N caused the precipitation of $[Cd(pz)_2]_n$ in an analytically pure form. Presumably, the intermediacy of an ionic tetrapyrazole cadmium complex, $[Cd(Hpz)]Cl_2$ avoids the formation of the hydroxo/pyrazolate species observed when $[Cd(Hpz)_2Cl_2]$ was present. Such complex behavior of the Cd^{II}/pyrazole system is also reflected by the incomplete analytical data and spectroscopic characterization attempted by Vos et al.[12a] and Das et al.[12b]

Mercury. When an acetonitrile solution of $Hg(NO_3)_2$ was treated with Hpz (Hg/Hpz = 1:3) the formation of a species analyzed as $Hg(pz)(NO_3)$, **3**, was observed (eq 6):

$$Hg(NO_3)_2 + Hpz \rightarrow Hg(pz)(NO_3) + HNO_3 \quad (6)$$

Noteworthy, the deprotonation of the pyrazole molecule to the pyrazolato group takes place without the need of any deprotonating agent. This behavior was already observed in the presence of a soft metal like silver.[24a] The full crystallographic characterization of **3** was performed by means of XRPD (see below) revealing the polymeric ionic nature of the species and the absence of short Hg−O contacts. Therefore, as will be explained below, a more suitable formulation of **3** is $[Hg(pz)]_n(NO_3)_n$.

When Et_3N was added to the reaction medium, a different species, analyzed as $Hg(pz)_2$, **4**, was isolated (eq 7). As revealed by the crystallographic study (see below), crystals of **4**, in contrast with the zinc and cadmium analogues, can be best

(22) Van Ooijen, J. A. C.; Van der Put, P. J.; Reedijk, J. *Chem. Phys. Lett.* **1977**, *51*, 380−382.

(23) That the reaction depicted in eq 2 does not occur in a single step is also confirmed by closely overlapping events traceable in the DSC and TGA analyses.

(24) See for example: (a) Ardizzoia, G. A.; La Monica, G.; Cenini, S.; Moret, M.; Masciocchi, N. *J. Chem. Soc., Dalton Trans.* **1996**, 1351−1357. (b) Masciocchi, N.; Ardizzoia, G. A.; LaMonica, G.; Moret, M.; Sironi, A. *Inorg. Chem.* **1997**, *36*, 449−454. (c) Burger, W.; Strähle, J. Z. *Z. Anorg. Allg. Chem.* **1986**, *539*, 27−33. (d) Carmona, D.; Oro, L. A.; Lamala, M. P.; Elguero, J.; Apreda, M. C.; Foces-Foces, C.; Cano, F. H. *Angew. Chem., Int. Ed. Engl.* **1986**, *25*, 1114−1116.

(25) Reedijk, J. *Rec. Trav. Chim.* **169**, *88*, 1451−1460.

(26) (a) Ehlert, M. K.; Rettig, S. J.; Storr, A.; Thompson, R. C.; Trotter, J. *Can. J. Chem.* **1990**, *68*, 1494−1498. (b) For a cobalt analogue see: Ehlert, M. K.; Rettig, S. J.; Storr, A.; Thompson, R. C.; Trotter, J. *Can. J. Chem.* **1993**, *71*, 1425−1436.

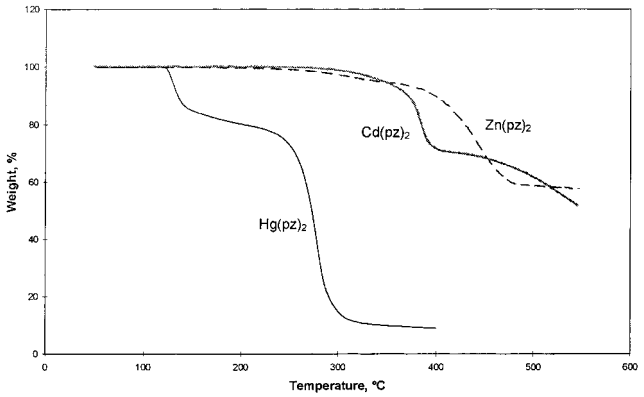

Figure 3. TGA traces for $[Zn(pz)_2]_n$, **1**, $[Cd(pz)_2]_n$, **2**, and $Hg(pz)_2$, **4**.

described as containing weakly interacting (nonpolymeric) mononuclear species.

$$Hg(NO_3)_2 + 2\,Hpz \xrightarrow{Et_3N} Hg(pz)_2 + 2(Et_3NH)NO_3 \quad (7)$$

Thermal Behavior of 1, 2, 3, and 4. The thermal stability of these pyrazolato species has been investigated by TGA (see Figure 3), DSC, and *preparative* thermal treatments. Compound **1** is a rather stable species, which can be heated to 440 °C without decomposition; at this temperature, a severely endothermic reaction occurs ($\Delta H \approx 220$ kJ mol^{-1}), forming the stable ($T_{dec} \approx 800$ °C[27]) $Zn(CN)_2$ compound in a highly crystalline form[28] and extruding CH_3CN molecules (GC−MS evidence). For the sake of comparison, the $[Zn(dmpz)_2]_n$ polymer was found to decompose at ≈ 300 °C,[26a] thus implying that it may adopt a different structure, possibly in order to minimize the heavy overlap of methyl groups from pyrazolate ligands attached to the same metal. Species **2** decomposes at lower temperatures (≈380 °C) than **1** but, owing to the much lower stability of its dicyanide ($T_{dec} \approx 200$ °C), the formation of acetonitrile is accompanied by reduction to metallic cadmium and cyanogen evolution; such a decomposition path is therefore similar to that suffered, near 320 °C, by $Hg(CN)_2$.[27]

A more complex thermal behavior is associated with $Hg(pz)_2$. Pyrazole is released near 140 °C as colorless needles; on the basis of analytical, TGA, and spectroscopic data, the remaining white (amorphous) powder is tentatively given a $[Hg(C_3H_2N_2)]_n$ formulation, particularly because its IR pattern is very similar to that of **4**, with the notable exception of one missing strong band near 1418 cm^{-1}. Such hydrogen abstraction might be accompanied by ring-C-mercuriation, as observed, for example, for the reaction between Hdmpz and $HgCl_2$,[29] preventing, therefore, the formation of the $Hg(CN)_2$ species; consistently, further heating does not show any decomposition near 320 °C (see above), nor formation of a (known to be unstable) Hg(CN) complex, a slowly varying loss of material being observed up to 400 °C. In addition, we also tried to thermally characterize the mixed-ligand species **3**; upon heating at about 250 °C, NO_2 is clearly evolved ($\Delta H \approx -40$ kJ mol^{-1}) and an intractable and *amorphous* dark-red powder was obtained.

Crystal Structures: The Zn and Cd Derivatives. The crystal structure determination from XRPD data clearly revealed the polymeric nature of complexes **1** and **2** (see Figure 4); one-dimensional chains of tetrahedrally coordinated metal atoms, bridged by μ-pz ligands, run along [001], the intermetallic distance being determined by *c*/2 value (3.69 and 3.96 Å, for **1** and **2**, respectively). In both cases, metals sit on a high-symmetry (*222)* position, while all pyrazolato ligands are bisected by a mirror plane (normal to *c*) passing through the midpoint of the N−N vector and the C(4) position. Therefore, only a single independent M−N interaction occurs, which was refined at 1.970(7) and 2.24(1) Å, for **1** and **2**, respectively.

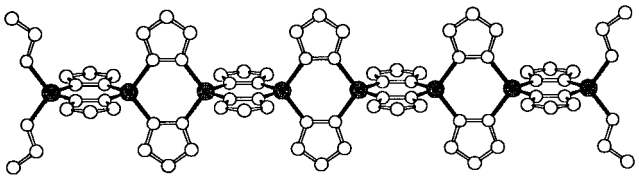

Figure 4. Drawing of a portion of the polymeric $[Zn(pz)_2]_n$ chain. Metal atoms are shaded and H atoms are not shown. The isomorphous $[Cd(pz)_2]_n$ phase looks, at the drawing resolution, similar.

On the basis of the final coordinates, it is possible to conclude that the isomorphous character of the zinc and cadmium derivatives can also be extended to the previously reported $[Cu(4X\text{-}pz)_2]_n$ series (4X−Hpz = 4-substituted pyrazole; X = H, CH_3, Cl, Br).[30] However, as briefly reported in synoptic Table 2, where the most relevant geometric features of species **1**, **2**, and $[Cu(4X-pz)_2]_n$ are collected, the high(er) tendency of Cu^{II}, than Zn^{II} or Cd^{II}, toward a more flattened (square-planar) coordination results in large differences in the N−M−N angles, those of the copper derivatives heavily deviating from ideal tetrahedral MN_4 coordination; additionally, very uniform M···M values are observed for the four different Cu^{II} species (3.85−3.89 Å), while a much shorter intermetallic distance is found for **1** (3.69 Å). Accordingly, the isomorphous character between **1** and $[Cu(4H-pz)_2]_n$, was detected only a posteriori, since the packing environments of the zinc and copper chains result in rather different unit cell parameters, but identical space group symmetry and topology. These results confirm, again, the high versatility of the pyrazolato ligand, which can bridge metal atoms at a variety of distances, depending on the geometric requirements of each metal center.[31]

All species reported in Table 2 possess chains *pseudo*hexagonally packed, in the [*hk*0] plane, by van der Waals (mostly H···H and, for Cu^{II} species, H···X) contacts. If an eccentricity value ϵ is evaluated ($\epsilon = 1 - [(a^2 + b^2)/a^2]^{1/2}/2$; $\epsilon = 0$ for ideal hexagonal packing), values of ca. 12, 8.6, and 0.4% can be computed for $[Cu(pz)_2]_n$, **1**, and **2**, respectively. It is worthy of note that the very small ϵ value observed for the $[Cd(pz)_2]_n$ species, together with the *odd* coincidence of *a*, *c*, and, as discussed, $(a^2 + b^2)/2$ (7.86, 7.92, and 7.88 Å, respectively), apparently simplifies the powder pattern, but may unpredictably affect its R_F factor, which requires the difficult partitioning of many reflections underlying the same observed peak (i.e., those sharing a common $h^2+3k^2+l^2$ value).

Crystal Structures: The Mixed-Metal Species. Since the copper, zinc, and cadmium pyrazolates are strictly isomorphous,

(27) Trotman-Dickerson, A. F. *Comprehensive Inorganic Chemistry*; Pergamon Press: Oxford, UK, 1973.

(28) Indeed, it is known that $Zn(CN)_2$ can be prepared from zinc powder and nitrogen-containing organic molecules.

(29) (a) De Luca, G.; Panattoni, C.; Renzi, G. *Tetrahedron*, **1976**, *32*, 1909−1910. (b) Cingolani, A.; Lorenzotti, A.; Leonesi, D.; Bonati, F. *Inorg. Chim. Acta* **1984**, *81*, 127−134.

(30) (a) Ehlert, M. K.; Rettig, S. J.; Storr, A.; Thompson, R. C.; Trotter, J. *Can. J. Chem.* **1989**, *67*, 1970−1974. (b) Ehlert, M. K.; Storr, A.; Thompson, R. C.; Einstein, F. W. B.; Batchelor, R. J. *Can. J. Chem.* **1993**, *71*, 331−334. (c) Ehlert, M. K.; Rettig, S. J.; Storr, A.; Thompson, R. C.; Trotter, J. *Can. J. Chem.* **1991**, *69*, 432−439.

(31) Indeed, pyrazolato-bridged M···M distances as low as 2.35 Å (Barron, A. R.; Wikinson, G.; Motevalli, M.; Hursthouse, M. B. *Polyhedron* **1985**, *4*, 1131−1134.) and as high as 4.56 Å (Sakagami, N.; Nakahanada, M.; Ino, K.; Hioki, A.; Kaizaki, S. *Inorg.Chem.* **1996**, *35*, 683−688.) have been observed.

Table 2. Structural Data for Isomorphous (Orthorhombic, *Ibam*) $[M(4X\text{-}pz)_2]_n$ Species

	$[Cu(4H-pz)_2]_n$	$[Cu(4Me-pz)_2]_n$	$[Cu(4Cl-pz)_2]_n$	$[Cu(4Br-pz)_2]_n$	$[Zn(4H-pz)_2]_n$	$[Cd(4H-pz)_2]_n$
a, Å	7.917(1)	9.777(8)	9.152(6)	9.44(1)	7.48[a]	7.86[a]
b, Å	11.491(2)	12.630(8)	13.021(7)	13.32(2)	14.38	13.65
c, Å	7.778(1)	7.748(7)	7.734(8)	7.70(1)	7.38	7.92
V, Å^3	708	952	916	968	795	849
color	green	green	green	green	colorless	pale yellow
M···M, Å (*c*/2)	3.89	3.87	3.87	3.85	3.69	3.96
M−N, Å	1.957(2)	1.96	1.96	1.96	1.970(7)	2.24(1)
N−M−N, deg	94−139	94−139	94−140	92−141	109−111	99−120
$T_{dec,}$ °C	270	270	290	290	441	353

[a] Actual values and their e.s.d.'s are reported in Table 1.

we decided to investigate the possible formation of mixed-metal pyrazolates as (random) copolymers, i.e., to determine their mutual (solid-state) solubility.

Starting from an equimolecular amount of $Cu(ClO_4)_2$, $Zn(ClO_4)_2$, excess pyrazole, and aqueous NH_3, a highly insoluble green species was obtained, which was not (XRPD evidence) a mixture of the $[Cu(pz)_2]_n$ and $[Zn(pz)_2]_n$ phases nor an ordered copolymer of larger periodicity. Its quasi-amorphous XRPD pattern showed, however, a large peak near $2\theta = 8.4°$ (d = 10.5 Å), about 0.8° wide, indicating that some correlation is present. If Et_3N is used instead of aqueous ammonia, a similar XRPD pattern is observed, with the notable exception of the presence of four additional broad peaks, reminiscent of their parent (and isomorphous) structures. The refined lattice parameters for such $[(Cu,Zn)(pz)_2]_n$ species (a = 7.55 Å, b = 14.05 Å, and c = 7.45 Å) are closer to those of the $[Zn(pz)_2]_n$, than to the $[Cu(pz)_2]_n$ values; accordingly, we tentatively suggest that such violation of Vegard's law is related to the high(er) flexibility of Cu^{II}. Indeed, it is much easier to accommodate copper ions (capable of sustaining a number of different stereochemistries) in the $Zn(pz)_2$ crystal lattice, than to force heavy local distortion of zinc ions coordination. The above results also point out that the kinetics of the $[(Cu,Zn)(pz)_2]_n$ phase formation is responsible for the appearance of Bragg peaks, which are completely absent in the samples obtained using ammonia.

In a similar effort, a (very pale) yellow powder was obtained by reacting an equimolecular mixture of zinc and cadmium perchlorates with excess pyrazole. XRPD data clearly showed a crystalline pattern, which could be indexed by an I-centered orthorhombic cell (a = 7.69 Å, b = 14.34 Å, and c = 7.59 Å); therefore, such mixed-metal phase is isostructural to its end-members and the sharp diffraction peaks indicate that the (random) copolymer obtained does not experience strain or other crystal defects, as observed in the Cu/Zn case. Accordingly, the bis-pyrazolato-bridged M···M distance (3.80 Å = c/2) closely matches the average M···M value of the pure phases (3.82 Å).

Finally, a *deep blue* copper/cadmium mixed-metal phase was also prepared, but was found to possess a rather complex, so far uninterpreted, XRPD pattern. Interestingly, this new crystal phase demonstrates the lack of mutual solubility of $[Cu(pz)_2]_n$ and **2**, and, as suggested by its color, may contain copper atoms in a rather different geometric (square-planar?) environment, not compatible with the structural features determined for the pure end-members. Analogously, earlier attempts in doping zinc and cadmium pyrazolates with small amounts of cobalt showed[12a] that Co^{II} ions, very much like Cu^{II} in the present study, may 'dissolve' into **1**, but not in **2**.

Crystal Structures: The Hg Derivatives. Different from its lighter analogues, $Hg(pz)_2$, **4**, can be described, as a first approximation, as a *molecular* solid, containing discrete mono-

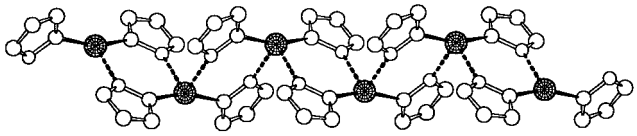

Figure 5. Drawing of a portion of the *pseudo*-polymeric $Hg(pz)_2$ chain. Metal atoms are shaded and H atoms are not shown. Fragmented bonds refer to loose Hg···N contacts (see text).

nuclear molecules packed in space by weak(er) *inter*molecular contacts (see Figure 5). That a discrete $Hg(pz)_2$ molecule, bearing two nearly linearly coordinated *mono*dentate pz ligands, exists, should not be surprising; similar examples can be found for mercury(II) halides and analogous species with N-donor ligands,[32] demonstrating the high tendency of Hg^{2+} ions toward bicoordination. However, a detailed analysis of the packing environment of the $Hg(pz)_2$ molecules clearly shows that the swinging ends of monodentate pz of (symmetry related) molecules lean toward neighboring metal centers, at distances for which Hg···N interactions cannot be neglected (ca. 2.5 Å, vs ca. 2.15 Å for Hg−N bonding contacts). This allowed, inter alia, the correct labeling of the C/N atoms next to the mercury-bonded N atom. Thus, a 1-D network of strong and weak(er) bonds extends throughout the crystals, running along *c*. That these ancillary ligands really participate in the coordination sphere of Hg(II) is also supported by the observed bending of the N−Hg−N angle [162.0(5)°, away from the two Hg···N contacts] and by the observation of the very poor solubility of species **4**. Therefore, the $Hg(pz)_2$ species can also be considered a coordination polymer built by bis-spiro[M−N−N−M−N−N−] rings, but, since the N−Hg−N angles heavily deviate from tetrahedral values (Hg being closer to a sawhorse geometry, with *cis*-N−H···N angles in the 88−108° range), the Hg atoms are not collinear anymore (Hg···Hg···Hg ca. 123°, see Figure 5).

On the basis of the above considerations, we expected the mixed pyrazolato-nitrato species **3** to be a structural analogue of **4**, i.e., a mononuclear species with, possibly, an extended (2-D or 3-D) network of Hg···O contacts throughout the crystal lattice. Surprisingly, our XRPD structure determination revealed the presence of polymeric $[Hg(pz)]_n^{n+}$ polycations, containing *exo*-bidentate pyrazolates and embedding NO_3^- groups at rather large distances from the mercury atoms (>2.70 Å, see Figure 6); such disposition, therefore, closely resembles that found in $Hg(OH)NO_3$,[33] where μ-OH bridges (Hg−O = 2.06 Å) of the $[Hg(OH)]_n^{n+}$ polycation show much stronger interactions with (bidentate) mercury ions than NO_3^- groups (Hg···ONO_2 > 2.66 Å). That the nitrato groups are not to be considered as part of the coordination sphere of mercury is also suggested by the

(32) Wells, A. F. *Structural Inorganic Chemistry*, 5th ed.; Clarendon Press: Oxford, UK, 1984.
(33) Ribar, B.; Matkovic, B.; Sljukic, M.; Gabela, F. *Z. Kristallogr.* **1971**, *134*, 311−318.

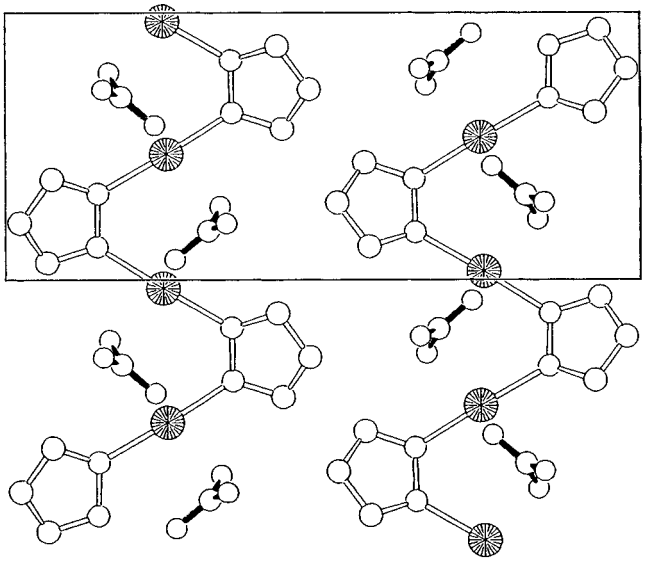

Figure 6. Drawing of portions of the polymeric $[Hg(pz)]_n^{n+}$ chains, [100] projection. Metal atoms are shaded and H atoms are not shown. The noncoordinating nitrates are also shown.

approximately linear [N−Hg−N 173(1)°] coordination geometry; within each chain, zigzagging throughout the crystal in the *c* direction (and winding up about a glide plane normal to *a*), the Hg atoms lie on an approximate straight line (Hg···Hg···Hg 178°) with pyrazolato ligands coplanar to each other; both such features differ in observation from the *strictly* topologically equivalent α-$[Cu(pz)]_n$ and $[Ag(pz)]_n$ chains,[6a] where bending at the Cu and Ag hinges occurs in order to avoid short H···H contacts, which, for large(r) intermetallic distances (Hg···Hg ca. 3.69 Å, vs Cu···Cu and Ag···Ag values of 3.16 and 3.40 Å, respectively) are more easily tolerated. On the basis of the observed structure, it might be possible that anion exchange in powders of $Hg(pz)NO_3$, soaked in concentrated saline solutions, occurs, but this chemical reactivity has not been investigated so far.

Conclusions

The present work has shown that on coupling selective synthetic procedures with spectroscopic, thermal, and, above all, powder diffraction analyses, it is possible to fully characterize a number of elusive polymeric species; the discovery and characterization of such thermally robust one-dimensional metal-containing polymers add new pieces of structural and chemical information, which are of interest in light of the recently reported anticorrosion properties of metal azolates.[34] With these aspects in mind, it is our goal to extend the reported synthetic and analytical experiments to further examples of coordination polymers, including different ligands, metals, and/or oxidation states. Indeed, preliminary work has shown that monophasic crystalline powders of Ni^{2+} and $[Hg_2]^{2+}$ pyrazolates, *not* isostructural with the species presented above, can be prepared; these will be discussed in a forthcoming paper.

In addition, we have illustrated how the isomorphous nature of the Zn and Cu species (which, apart from the similarity of the cell parameters and the identity of the space group symmetry operations, in the single-crystal case would be evident at a glance, once the 3-D *hkl* intensity distributions are compared), on using XRPD data can be somewhat obscured, owing to the 1-D projection of the reciprocal space into the 2θ dimension. That is, powder diffraction peaks, sorted on ascending d^* values, may occur in rather scrambled positions, even if (roughly) maintaining similar F's; as a consequence, what is considered a 'structural fingerprint' cannot be easily recognized as such if lattice parameters suffer anisotropic inflation (or, as in the present case, changes of signs). Accordingly, the isomorphous character of the copper, zinc, and cadmium species was also missed in previously reported XRPD work,[12a] confirming that a complete structural analysis (solution and refinement) is mandatory in order to certify simple, but important, structural features.

Acknowledgment. We thank the Italian Consiglio Nazionale delle Ricerche and MURST for funding. We also acknowledge financial support from ICDD, International Centre for Diffraction Data.

Supporting Information Available: Full list of fractional atomic coordinates, bond distances and angles for compounds **1**, **2**, **3**, and **4**. This material is available free of charge via the Internet at http://pubs.acs.org.

IC990258U

(34) (a) Richmond, W. N.; Faguy, P. W.; Weibel, S. C. *J. Electroanal. Chem.* **1998**, *448*, 237−244. (b) Tsarenko, I. V.; Chizhik, S. A.; Makarevich, A. V. *Protect. Met.* **1999**, *35*, 81−84.